TMRC-04-01

MDOT Research Report RC-1443

Petrographic Evaluation of Cores from the Mosel Avenue Bridge

Final Report

Submitted to the

Michigan Department of Transportation

By

Thomas Van Dam, Ph.D., P.E.
Principal Investigator
Karl R. Peterson
Larry L. Sutter, Ph.D.
Pedro Lemmertz

Transportation Materials Research Center
Michigan Technological University
Dept. of Civil and Environmental Engineering
1400 Townsend Drive
Houghton, MI 49931

March 31, 2004

1. Report No. Research Report RC-1443	2. Government Accession No.	3. MDOT Project Manager John Staton
4. Title and Subtitle Petrographic Evaluation of Cores from the Mosel Avenue Bridge		5. Report Date April 2004
7. Author(s) T.J. Van Dam, K.R. Peterson, L.L. Sutter, and P. Lemmertz		6. Performing Organization Code
9. Performing Organization Name and Address Michigan Technological University 1400 Townsend Drive Houghton, Michigan 49931		8. Performing Org Report No. TMRC-04-01
12. Sponsoring Agency Name and Address Michigan Department of Transportation Construction and Technology Division P.O. Box 30049 Lansing, MI 48909		10. Work Unit No. (TRAIS) 11. Contract Number: 11(a). Authorization Number:
15. Supplementary Notes		13. Type of Report & Period Covered 14. Sponsoring Agency Code

16. Abstract
The early deterioration of the concrete sidewalk on the Mosel Avenue bridge located in Parchment, Michigan near Kalamazoo was investigated. Core specimens obtained through the sidewalk into the deck were evaluated petrographically to determine the cause of the deterioration. The cause of deterioration of the concrete in the sidewalk and deck is related to deleterious alkali-silica reaction of the reactive particles in the fine aggregate. It is obvious that the chert constituent in the fine aggregate is providing the reactive silica necessary to fuel the alkali-silica reaction. But for this reaction to occur, the total alkalis in the mixture must be high enough to initiate and drive the reaction. Although the deck appeared to be free of distress, microscopically it was similarly affected. In the case of the sidewalk, the poor curing and lack of reinforcement allowed ready ingress of water, unrestrained swelling of the alkali-silica reaction product, and cracking. Once cracking occurred, the integrity of the concrete was compromised, and pathways for the ingress of water and deicing chemicals were created. As this water saturated the weakened concrete and froze, further damage from ice formation may have hastened the deterioration.

17. Key Words concrete deterioration, freez-thaw deterioration, alkali-silica reactivity	18. Distribution Statement No restrictions. This document is available to the public through the Michigan Department of Transportation.		
19. Security Classification (report) Unclassified	20. Security Classification (Page) Unclassified	21. No of Pages 24	22. Price

Introduction

It was observed that the Mosel Avenue bridge located in Parchment, Michigan near Kalamazoo was undergoing some unexpected distress, with the sidewalk suffering severe deterioration. Figure 1 shows the condition of the sidewalk on the western portion of the north side of the bridge. A total of four 100-mm diameter cores were obtained through the sidewalk and into the deck and sent to Michigan Tech for examination. Each core included the full depth of the sidewalk (approximately 250 mm) and approximately 80 mm of the underlying deck concrete. The cores labeled "1" and "2" came from the north fascia sidewalk of the bridge at a distance of 0.9 m from the curb. The cores labeled "3" and "4" came from the south fascia sidewalk of the bridge at a distance of 0.3 m from the curb.

Figure 2 shows the cores as retrieved from the south fascia sidewalk of the bridge. Both demonstrate cracking planes oriented parallel to the pavement surface throughout the depth of the cores. The deformed reinforcing bar at the base of the deck portion of core "4" shows no sign of corrosion. Figures 3 and 4 show polished slabs cut from the cores retrieved from the north fascia sidewalk of the bridge. The slabs show cracks running sub-parallel to the pavement surface as well as from the surface downward vertically into the cores. To enhance the appearance of the air voids and cracks, the polished slabs were colored black and a very fine white powder was forced into the air voids and cracks. The negative images (air voids and cracks appear black) are presented on the right side of figures 3 and 4. Figures 5 through 10 show more highly magnified images of the same slabs. A modified point count was performed in accordance with *ASTM C 457 Standard Test Method for Microscopical Determination of Parameters of the Air-Void System in Hardened Concrete* on the polished slabs from cores "1" and "2", both for the sidewalk concrete and for the concrete obtained from the deck. Thin sections were prepared from core "2" and examined with a petrographic microscope and a scanning electron microscope.

Slabs from cores "1" and "2" were also crushed, and an extraction performed to determine the available sodium and potassium in terms of kg of Na_2O equivalent (Na_2O + 0.658 K_2O) per m^3 of concrete. The total amount of sodium and potassium in the mixture

influences the pH of the pore solution, which in turn affects the solubility of the siliceous constituents in the aggregates. Thus, the potential for the aggregate to react is directly related to the total alkalinity of the mixture. The cement alkalinity is one factor that contributes to this measure of total alkalinity, but it there are other factors as well. For example, two mixtures made with the same cement will have different total alkalinity if one of the mixtures has higher cement content. In addition, other concrete constituents, including some supplementary cementitious materials, can contribute alkalis to the mix. All these factors must be accounted for to fully understand the potential for alkali-silica reactivity. For this reason, it is not enough to focus only on the alkalinity of the cement, but instead the total alkalinity of the mixture as measured in terms of kg of Na_2O equivalent per m^3 must be calculated.

Stereo Optical Microscope Evaluation

The polished slabs were viewed with a stereo optical microscope to conduct ASTM C 457 and make some general observations of the concrete microstructure. The results of the air-void system analysis are summarized in table 1. Both the sidewalk and the deck have adequate air-void system parameters for freeze-thaw protection. Infilling of air voids by ettringite and alkali-silica reaction products is minimal. During the stereo optical air-void system analysis, observations were made of reactive chert fine aggregate particles. Figures 11 and 12 show stereo microscope images of the chert fine aggregate particles associated with cracking from the sidewalk and deck portions of polished slabs from core "2". The cracks are empty some distance from the chert particles, but are filled with alkali-silica reaction products in the immediate vicinity of the chert particles. All of the cracks exposed on the polished slabs, whether from the sidewalk or deck, intersected reactive chert particles, suggesting a "connect-the-dots" pattern between the reacting chert particles.

Petrographic Analysis

Thin sections were prepared from core "2" to confirm the presence of alkali-silica reaction products. Figure 13 shows a crack that intersects several reactive fine aggregates that contains deposits of alkali-silica reaction products. Figure 14 shows further close-

ups of the reactive chert particle from the upper left hand corner of figure 13. Figure 15 shows backscatter electron images of the alkali-silica reaction product from the same chert particle. The alkali-silica reaction product contains both amorphous and crystalline bladed phases. Figure 16 shows elemental maps of the same area shown in figure 15. The alkali-silica reaction product contains silicon, calcium, potassium, and sodium.

Alkali Extraction

Slabs from cores "1" and "2" were crushed and extractions performed to measure available sodium and potassium using a pH neutral ammonium acetate extractant. Approximately 50 grams of crushed concrete powder was used for each extraction. The powder was immersed in the ammonium acetate solution, then filtered and further rinsed to collect 500 ml of filtrate. The filtrate was evaporated to dryness, and fired in a muffle furnace at 400 °C for a period of thirty minutes. The resulting ash was pulverized and treated with hydrochloric acid, then filtered and rinsed with water to collect 50 ml of filtrate. Sodium and potassium concentrations were determined by inductively coupled plasma emission spectrometry.

To convert the sodium and potassium concentrations to units of kg Na_2O per m^3 of concrete, the unit weight of the concrete must be known. Since construction records were not available, bulk density after immersion values, determined according to ASTM C 642, were substituted. Bulk density after immersion values were found to be 2308 kg/m^3 for both the sidewalk and bridge deck. The results of the extraction procedure are summarized in table 2, and in displayed graphically in figures 17 and 18. In order to assess the efficiency of the extraction procedure, extractions were also performed on mortar cylinders of 0.40, 0.50, and 0.60 w/c made with Ottawa 20-30 sand and Lafarge Type I Alpena cement with a Na_2O equivalent level of 0.51 wt%. The results of the extraction efficiency assessment are summarized in table 3, and in figure 19. Values for kg Na_2O equivalent per m^3 of mortar were computed using the mix design and the known cement alkali levels. As shown in table 3, the extraction procedure performed well at the 2.5 kg Na_2O level, only underestimating the computed alkali level by less than 0.1 kg. However, the extraction procedure underestimated the computed levels by larger margins as the computed alkali levels decreased. Based on this assessment, it should be noted that

the kg Na_2O per m^3 of concrete values determined by extraction might underestimate the true alkali levels.

As discussed, the analysis was performed to estimate the amount of alkalis available in the hydrated cement paste. Canadian standards suggest a maximum of 3.0 kg Na_2O equivalent per m^3 of concrete for mild protection against alkali-silica reaction. If moderately to highly reactive aggregates are present, the total alkalinity must be limited to less than 1.7 Na_2O equivalent per m^3 of concrete. As shown in table 2, the bridge deck, and the bottom half of the sidewalk from core "1" have extracted alkali values just above the 1.7 kg Na_2O equivalent limit. However, the top half of the sidewalk from core "1", and the entirety of core "2" have extracted alkali values that exceed the 3.0 kg Na_2O equivalent limit. In the case of the top half of core "1", and the entirety of core "2", it is likely that the heightened alkali levels are due to the ingress of deicers through the cracking network, and not related to the initial alkali levels of the concrete. The lower alkali levels of the bridge deck and bottom half of the sidewalk from core "1" are probably more representative of the concrete in its initial condition. Although the extracted alkali levels from the bridge deck and bottom half of the sidewalk from core "1" barely exceed the 1.7 kg Na_2O equivalent limit, as noted previously the extraction likely underestimates the true alkali level to a limited degree.

Conclusions

The cause of deterioration of the concrete in the sidewalk and deck is related to deleterious alkali-silica reaction of the reactive particles in the fine aggregate. It is obvious that the chert constituent in the fine aggregate is providing the reactive silica necessary to fuel the alkali-silica reaction. But for this reaction to occur, the total alkalis in the mixture must be high enough to initiate and drive the reaction. As discussed in this report, high alkali cement coupled with a high cement content will result in a high total alkali content of the concrete. In the presence of reactive aggregates, this is more damaging than if a low alkali cement coupled with low cement content was used. This can explain why a given aggregate can serve well in some mixtures but be reactive in others. Further, the use of other mitigating techniques including pozzolans or lithium admixtures can further reduce the occurrence of alkali-silica reactivity. And finally,

water is needed for the alkali-silica reaction product to swell and damage the concrete. Unfortunately, precipitation will provide all the moisture needed to drive a deleterious reaction. Yet concrete of low permeability will not likely manifest distress as quickly as that of relatively high permeability as the source of moisture will be limited.

It is interesting to note that although the sidewalk and deck appear to be made of the same materials and are both experiencing alkali-silica reaction, the sidewalk is in much worse condition. While the deck is not currently showing signs of visible deterioration as seen by the naked eye, the deck does show signs of alkali-silica reaction as seen by the microscope. Although it is only speculative, two hypotheses are forwarded to possibly explain the contrast in visible deterioration. The first is that the deck was moist cured after placement whereas the sidewalk was simply coated with a membrane forming curing compound. The wet curing would significantly reduce shrinkage cracking while promoting hydration, creating a relatively impermeable concrete. Even in the best of times, a membrane forming curing compound will only retain water already in the mixture, and will not provide the same degree of curing as does a wet cure. Concrete cured with a membrane forming curing compound would thus be expected to be more permeable strictly as a result of the less rigorous curing, and as discussed, a less permeable concrete will suffer deterioration more quickly.

The second hypothesis, which is likely working in conjunction with the first, is that the steel reinforcement in the deck is providing internal restraint to the expansion produced by the swelling alkali-silica reaction product. This restraint is keeping cracks very tight, reducing the ingress of moisture, and thus maintaining the integrity of the concrete.

In the case of the sidewalk, the poor curing and lack of reinforcement allowed ready ingress of water, unrestrained swelling of the alkali-silica reaction product, and cracking. Once cracking occurred, the integrity of the concrete was compromised, and pathways for the ingress of water and deicing chemicals were created. As this water saturated the weakened concrete and froze, further damage from ice formation may have hastened the deterioration.

Table 1: Results of air void analyses.

	core 1, sidewalk	core 2, sidewalk	core 1, deck	core 2, deck
Raw Data				
area analyzed (cm^3)	71.0	71.0	76.8	71.0
traverse length (mm)	3625.8	3625.8	3921.0	3625.8
air void stops	95	112	98	90
paste stops	434	366	474	490
aggregate stops	858	910	927	807
Secondary void infilling stops	1	0	2	1
total stops	1388	1388	1501	1388
air void intercepts	1392	2039	1823	1609
filled air void intercepts	17	6	17	5
Results				
vol% air (existing)	6.8	8.1	6.5	6.5
vol % air (original)	6.9	8.1	6.7	6.6
vol % paste	31.3	26.4	31.6	35.3
vol % aggregate	61.8	65.6	61.8	58.1
vol% secondary void infilling	0.1	0	0.1	0.1
existing spacing factor (mm)	0.198	0.117	0.16	0.176
existing paste/air ratio	4.58	3.27	4.86	5.46
existing air void specific surface (mm^{-1})	22.4	27.9	28.5	27.4
existing air void frequency (voids/m)	384	562	465	444
existing air void avg. chord length (mm)	0.178	0.143	0.14	0.146
original spacing factor (mm)	0.197	0.117	0.16	0.176
original paste/air ratio	4.52	3.27	4.74	5.38
original air void specific surface (mm^{-1})	22.5	28	28.2	27.2
original air void frequency (voids/m)	389	564	469	445
original air void avg. chord length (mm)	0.178	0.143	0.142	0.147

Table 2: Results of alkali extraction from cores

	Na (ppm)	K (ppm)	total alkalis (kg/m^3)	avg. total alkalis (kg/m^3)	std. dev. total alkalis (kg/m^3)
Core 1					
top half of sidewalk	157	911	4.21	4.2	0.08
	166	916	4.23		
	160	896	4.09		
bottom half of sidewalk	81	417	1.96	1.8	0.14
	71	389	1.81		
	65	366	1.68		
bridge deck	59	387	1.72	1.8	0.17
	71	441	1.97		
	60	378	1.66		
Core 2					
top half of sidewalk	150	1004	4.56	4.4	0.18
	127	942	4.21		
	137	952	4.32		
bottom half of sidewalk	107	911	3.93	4.2	0.31
	115	1062	4.56		
	113	974	4.24		
bridge deck	121	1147	4.92	4.9	0.18
	131	1169	5.04		
	109	1096	4.68		

Table 3: Results of extraction efficiency assessment.

	total alkalis (kg/m^3) from extraction	avg. total alkalis (kg/m^3) from extraction	total alkalis (kg/m^3) computed from mix design	difference between computed value and avg. extracted value
0.40 w/c mortar	2.42	2.44	2.53	0.09
	2.45			
0.50 w/c mortar	1.91	1.91	2.18	0.27
	1.92			
0.60 w/c mortar	1.25	1.25	1.95	0.70
	1.25			

Figure 1: North fascia sidewalk of Mosel Avenue bridge showing deterioration of sidewalk.

Figure 2: From left to right, cores "3" and "4" from the south fascia sidewalk of the Mosel Avenue bridge, scale bar measures 10 cm.

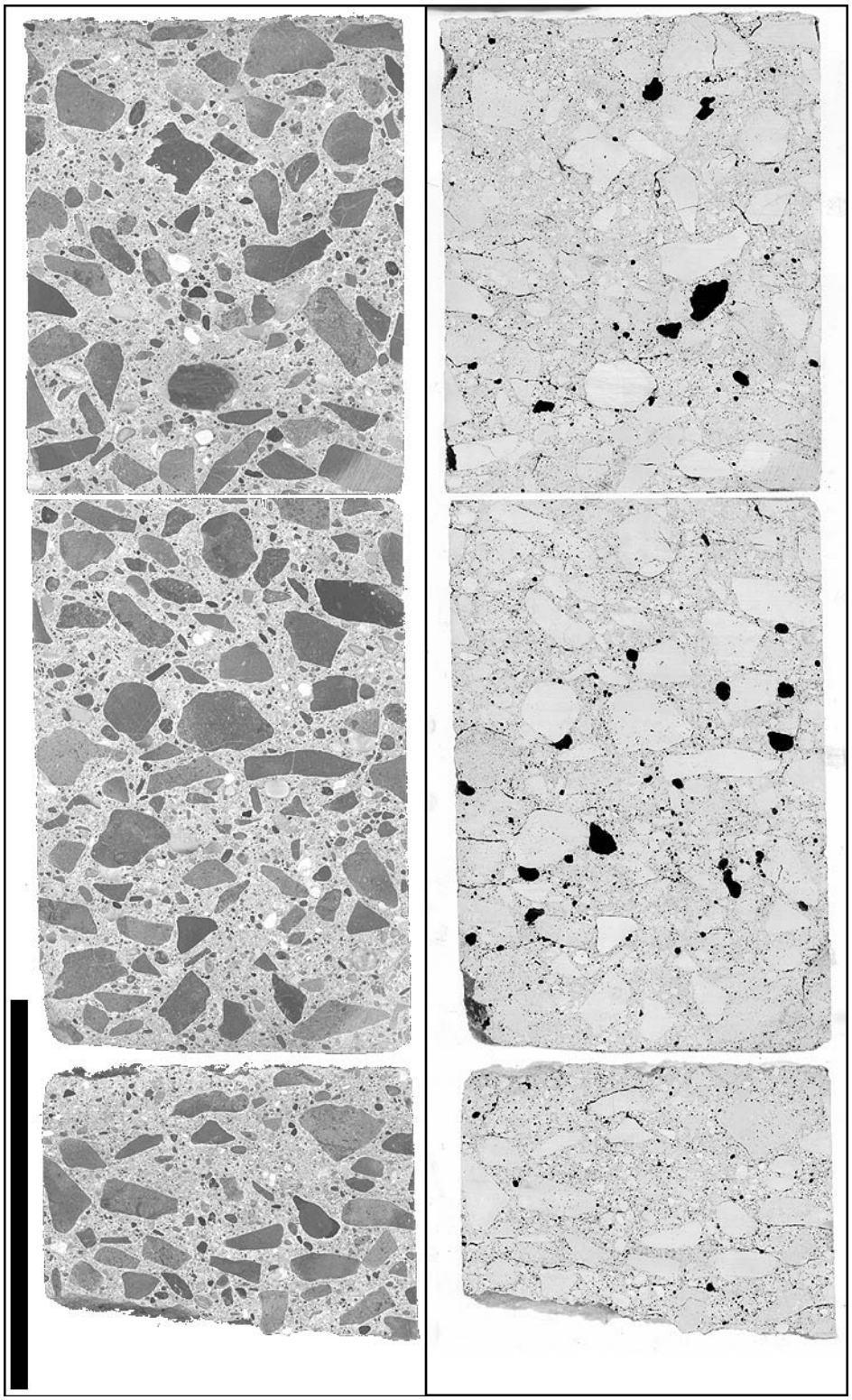

Figure 3: Polished slabs from core "1", left side shows slabs as-polished, right side shows slabs after treatment to enhance air voids and cracks, scale bar 10 cm.

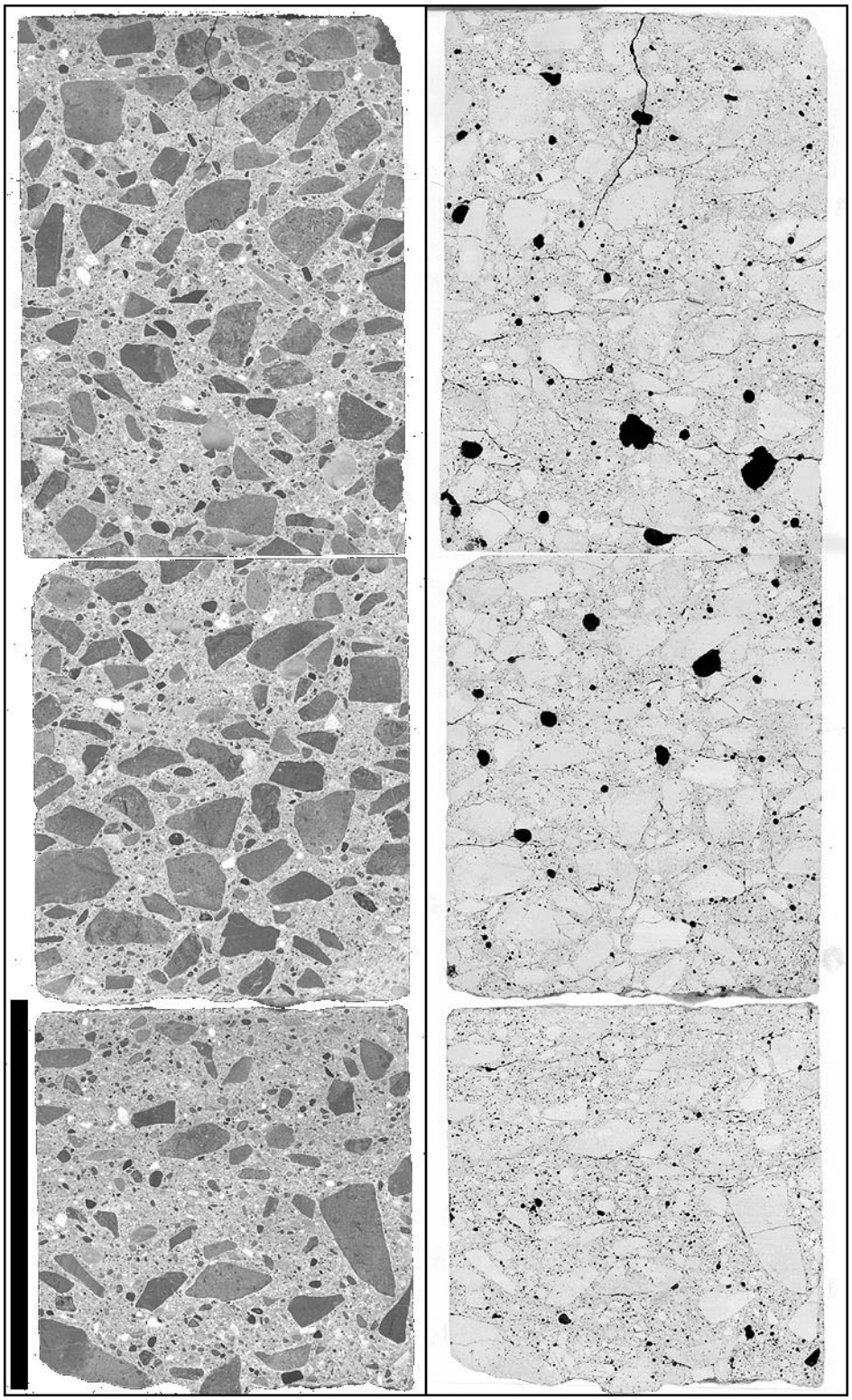

Figure 4: Polished slabs from core "2", left side shows slabs as-polished, right side shows slabs after treatment to enhance air voids and cracks, scale bar 10 cm.

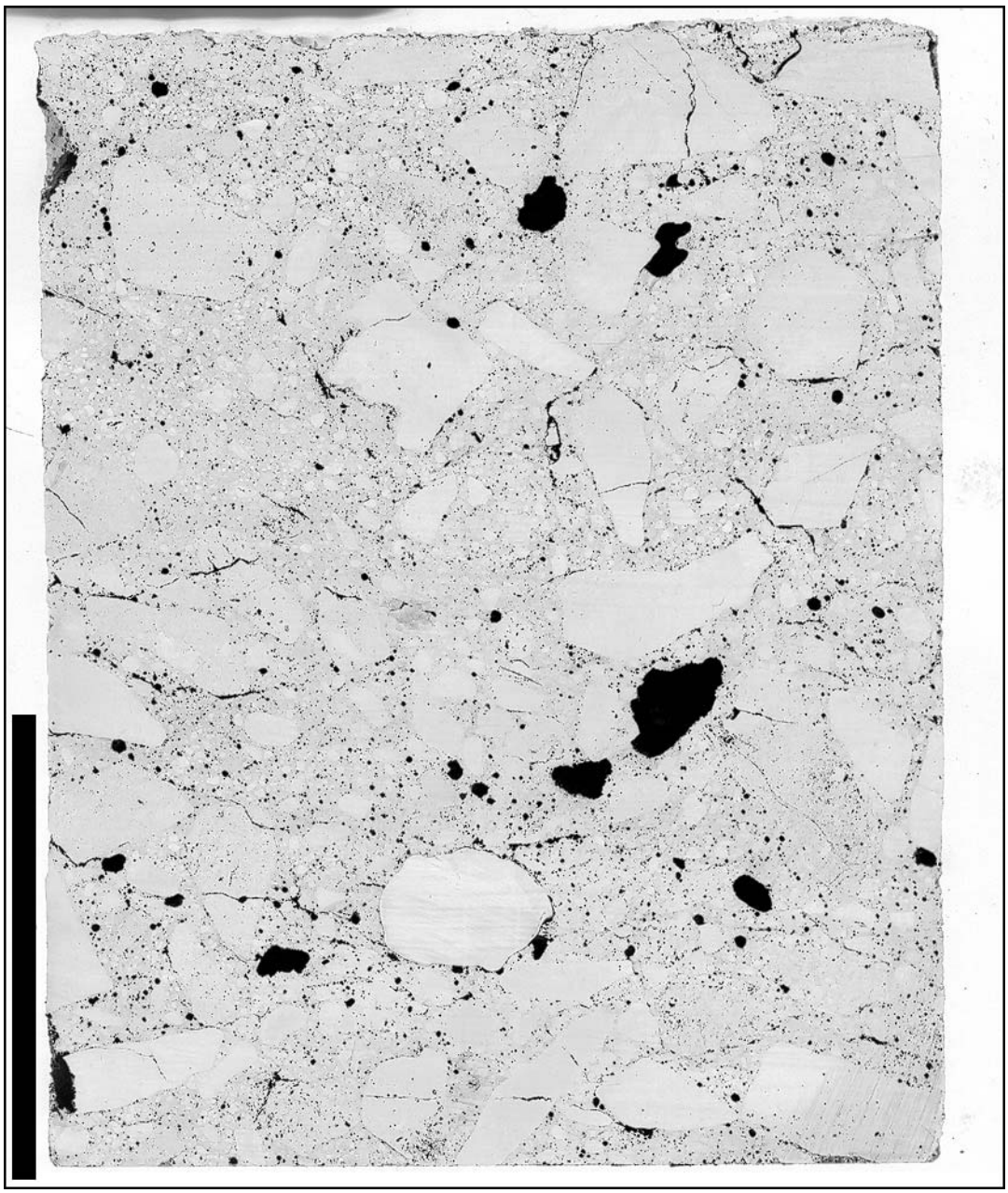

Figure 5: Close up of top half of sidewalk portion of core "1" to show cracks, scale bar 5 cm.

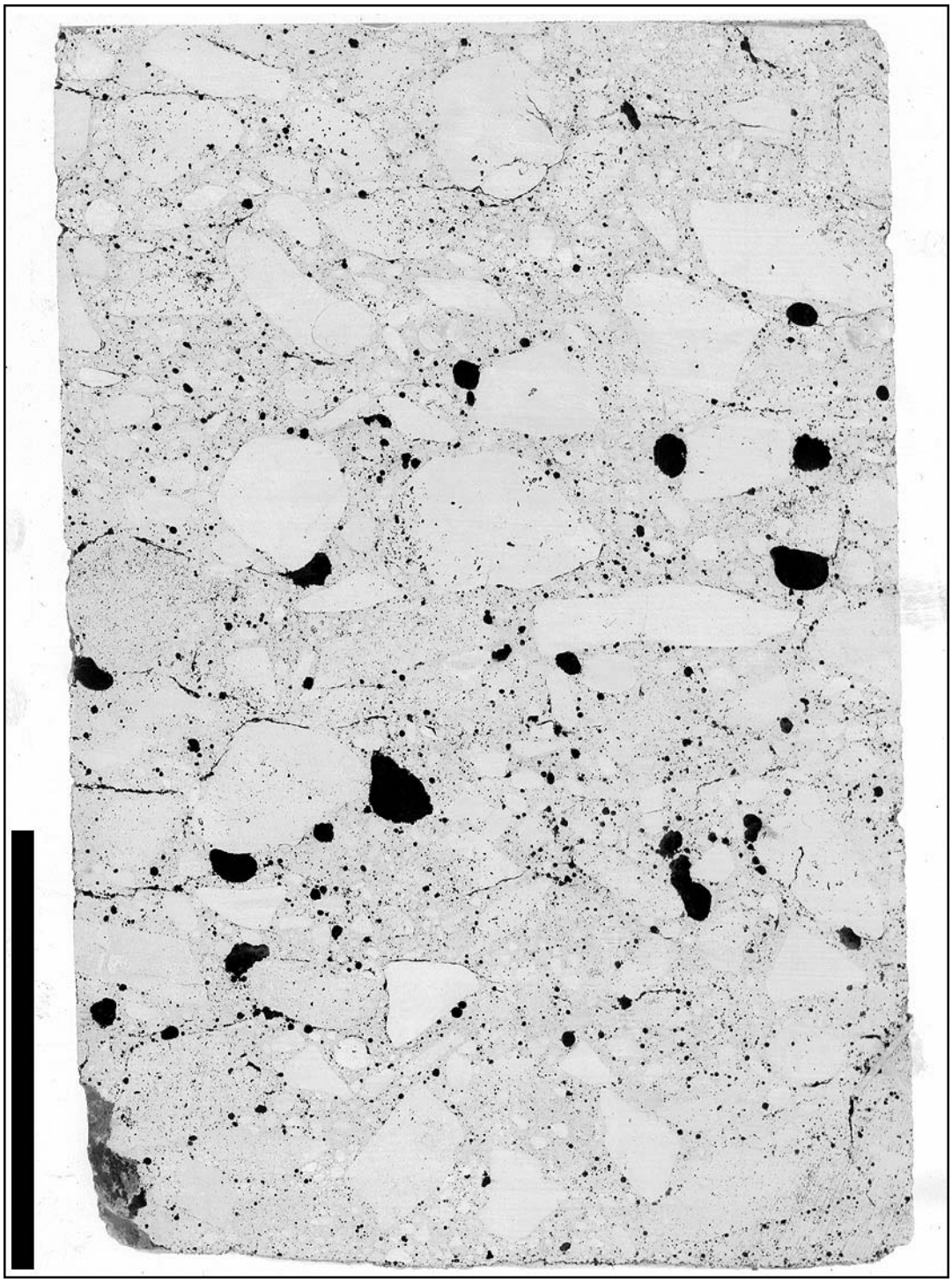

Figure 6: Close up of bottom half of sidewalk portion of core "1" to show cracks, scale bar 5 cm.

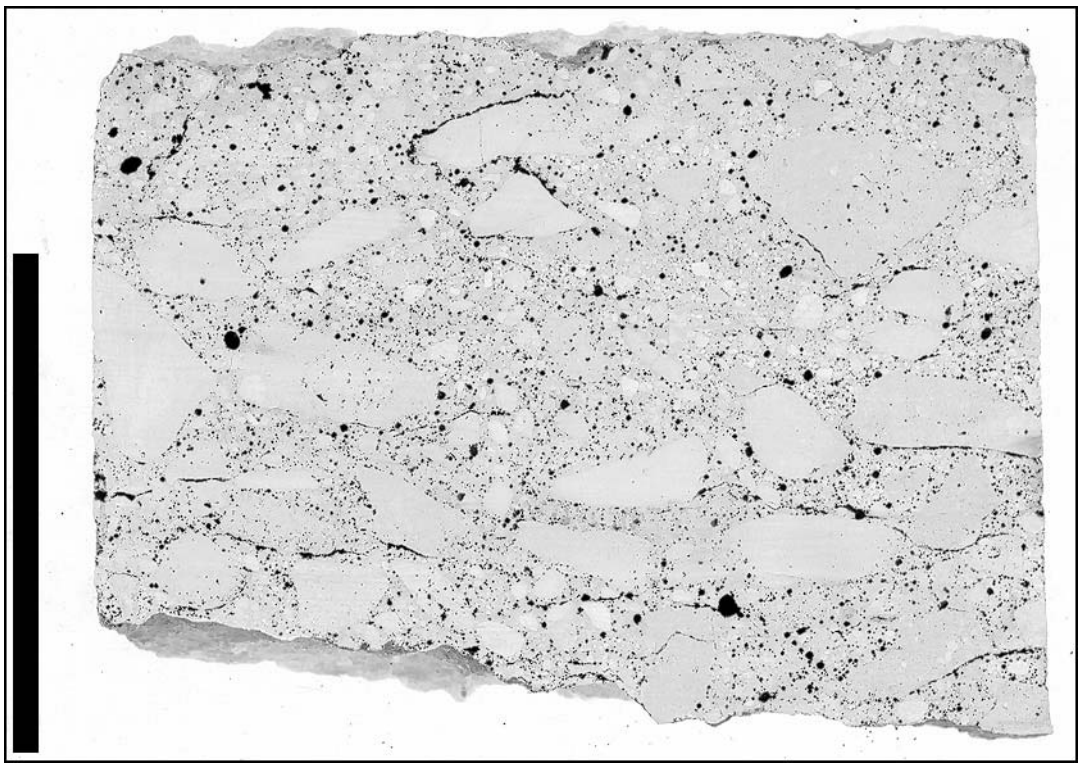

Figure 7: Close up of deck portion of core "1" to show cracks, scale bar 5 cm.

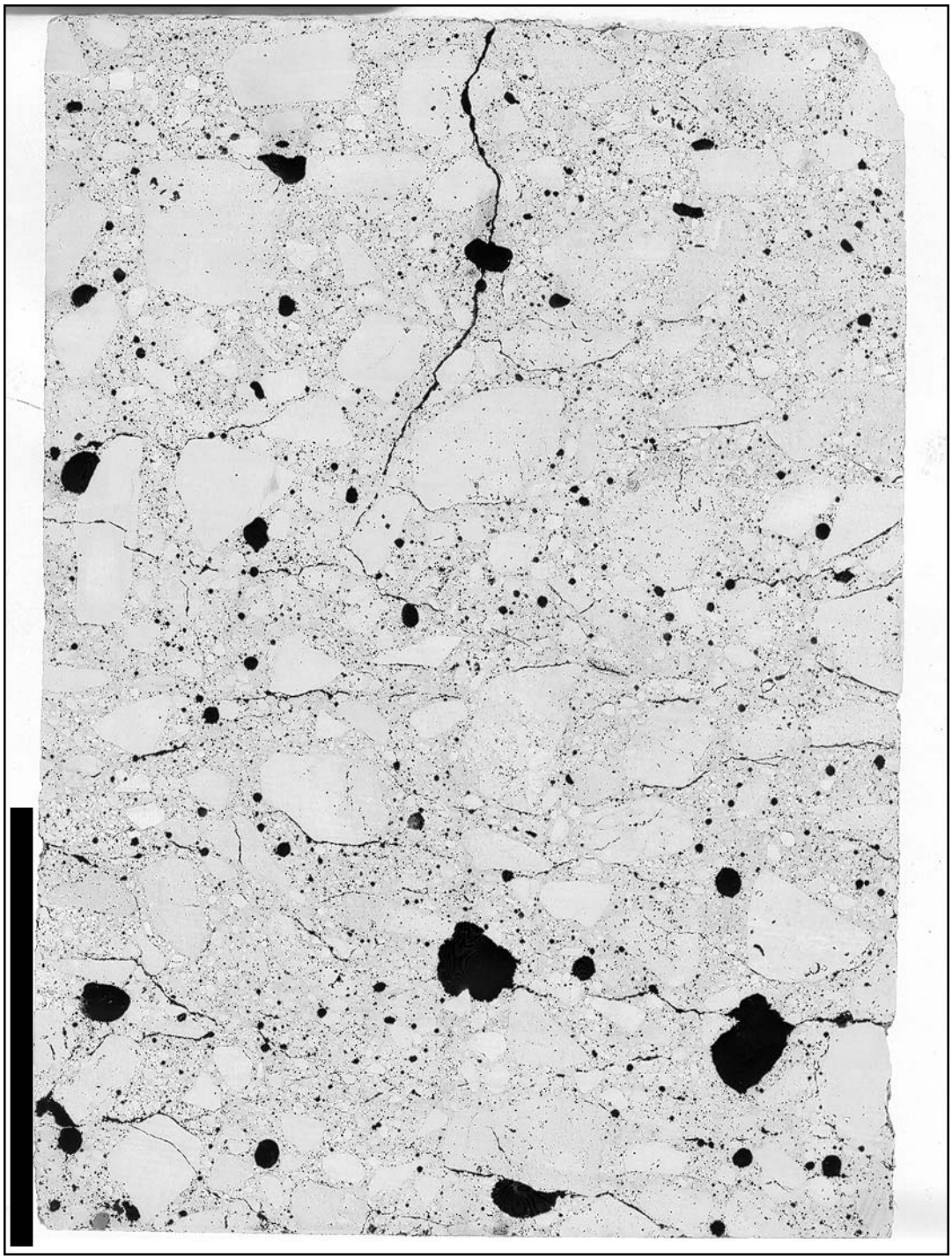

Figure 8: Close up of top half of sidewalk portion of core "2" to show cracks, scale bar 5 cm.

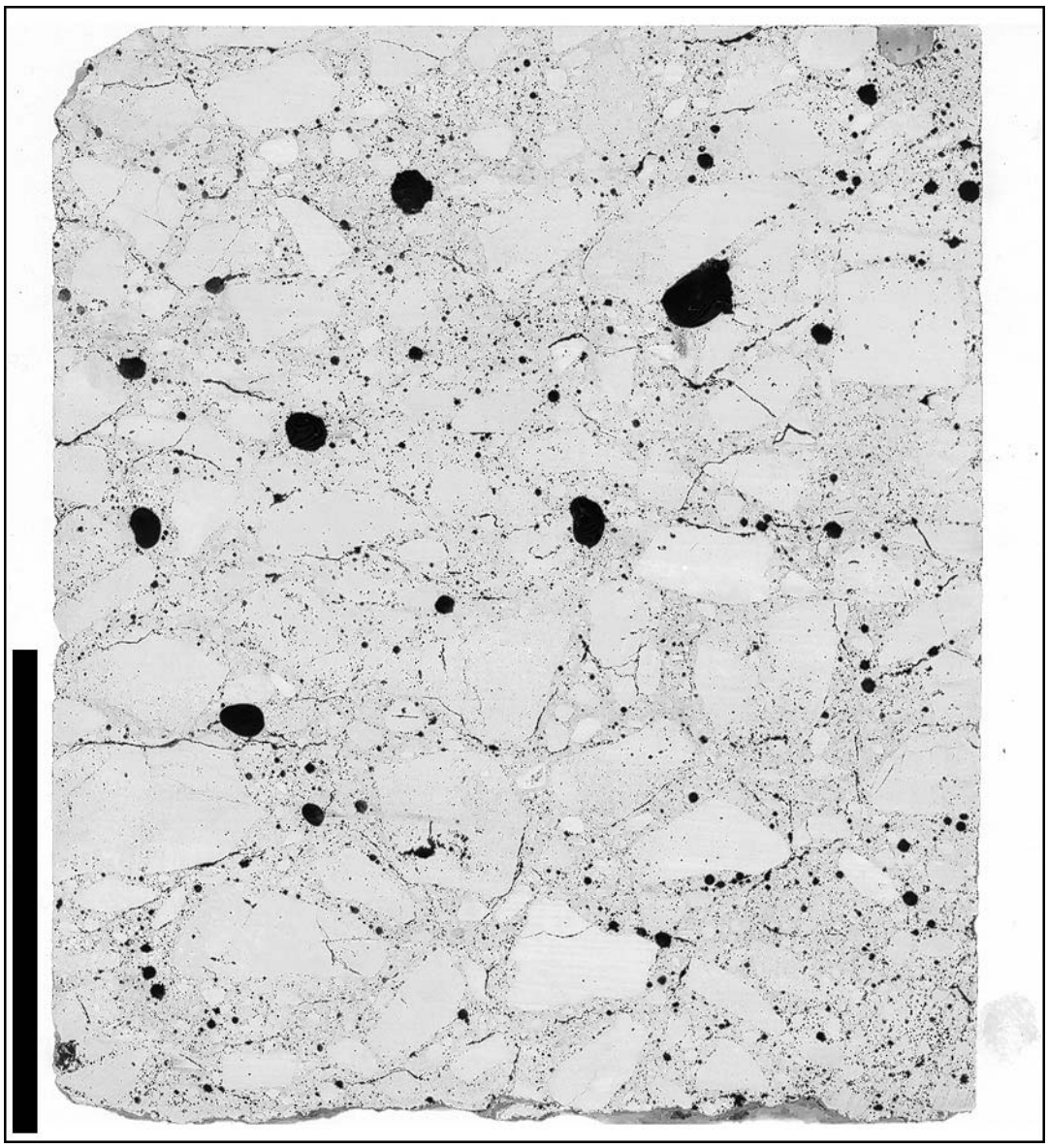

Figure 9: Close up of bottom half of sidewalk portion of core "2" to show cracks, scale bar 5 cm.

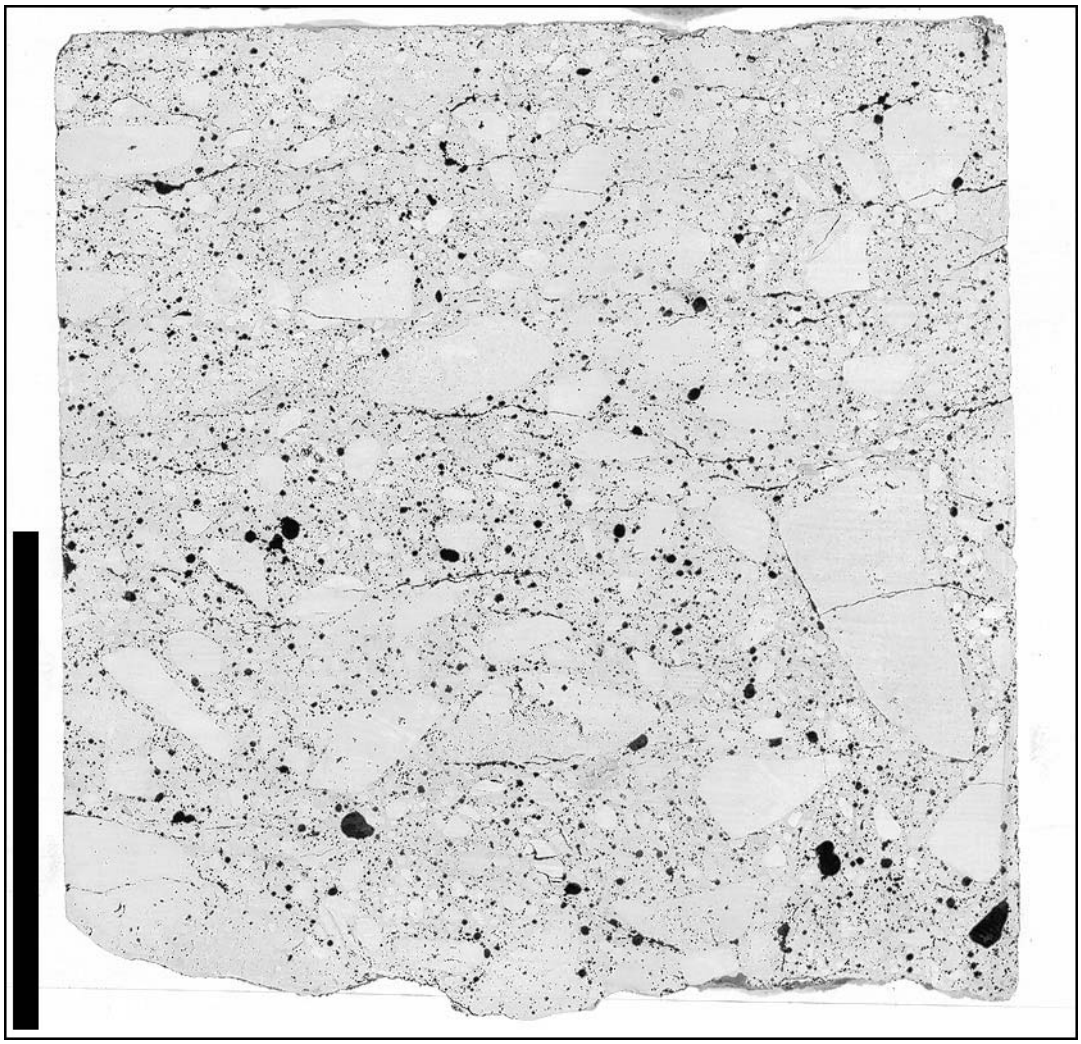

Figure 10: Close up of deck portion of core "2" to show cracks, scale bar 5 cm.

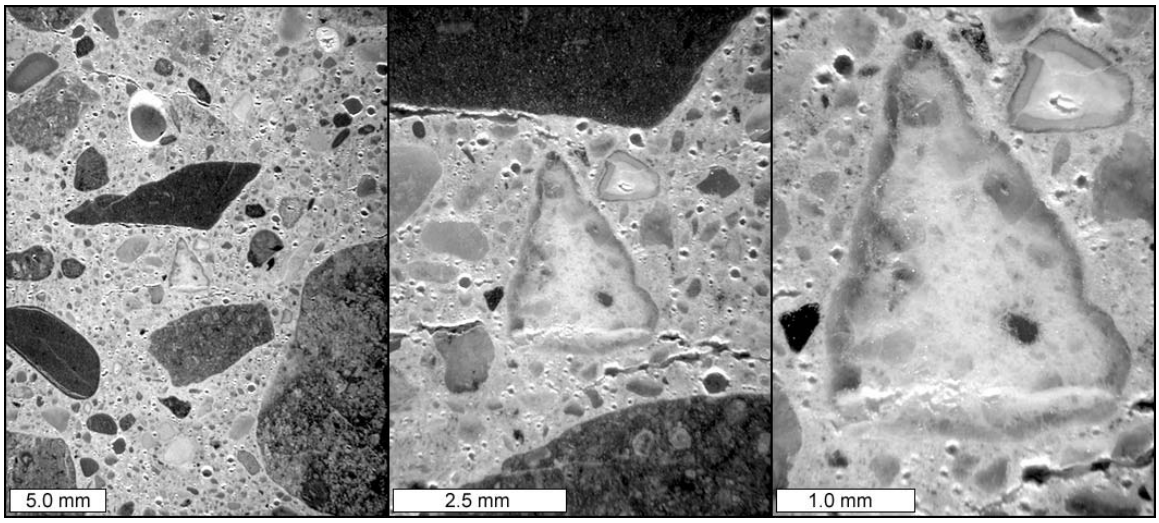

Figure 11: Stereo microscope images showing reactive chert on polished slab from sidewalk portion of core "2".

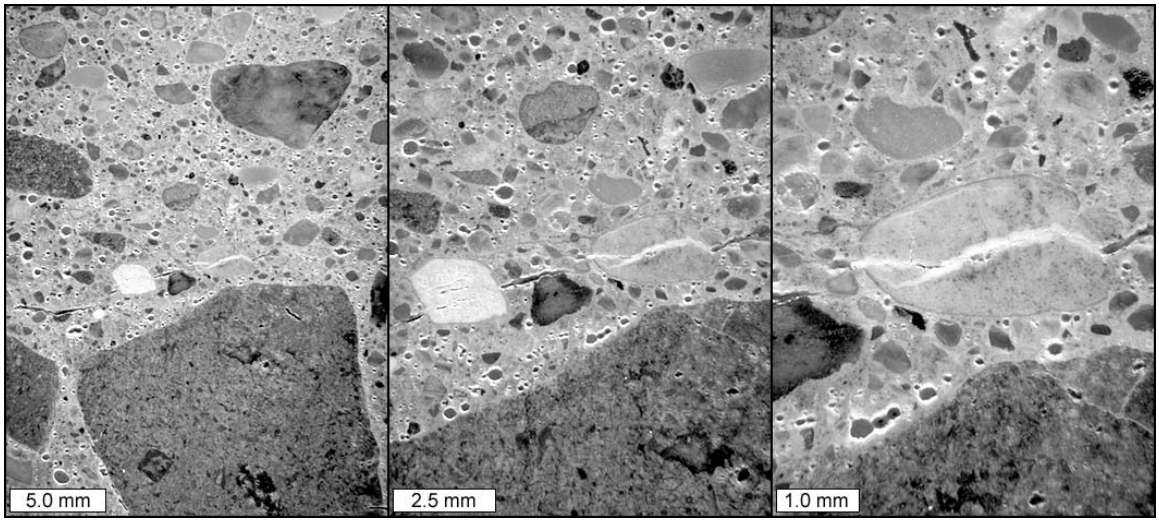

Figure 12: Stereo microscope images showing reactive chert on polished slab from deck portion of core "2"

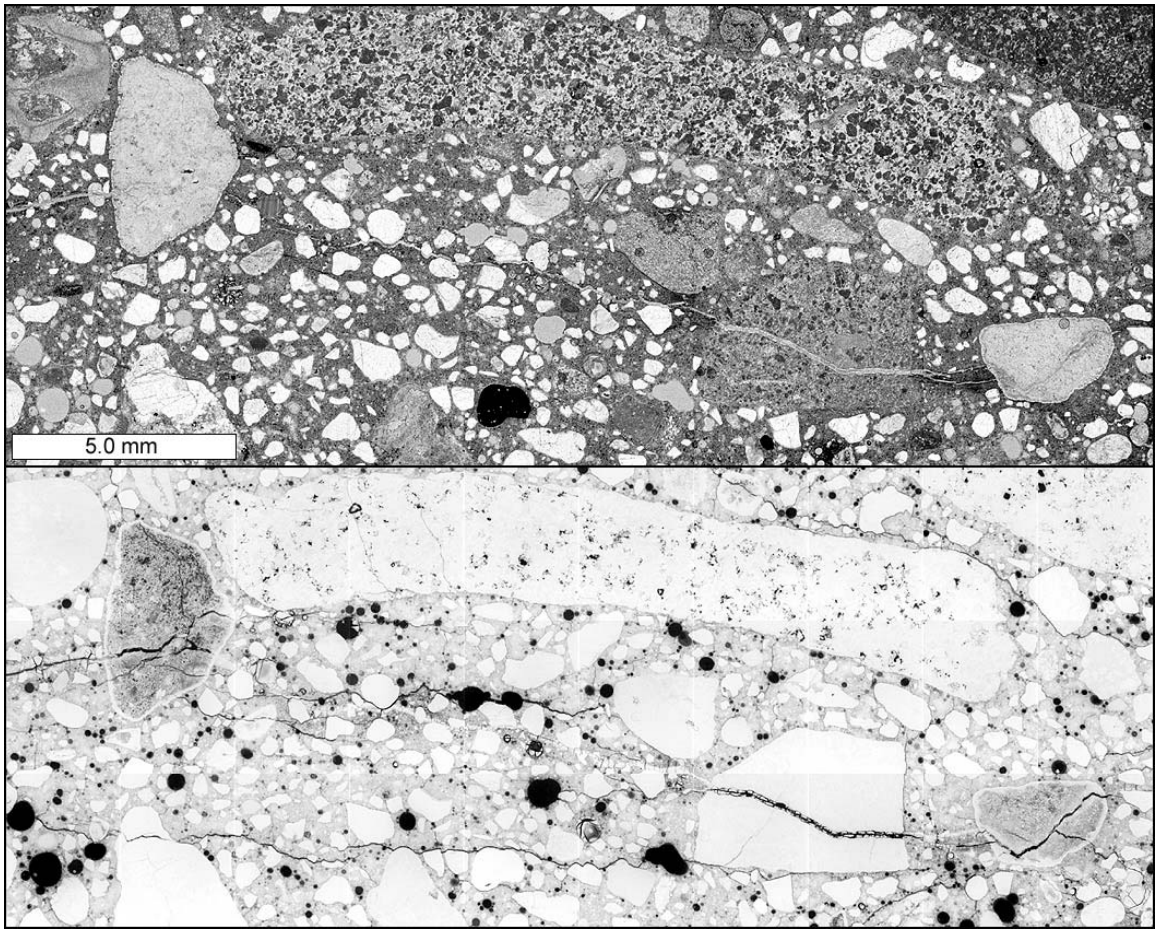

Figure 13: Petrogrpahic microscope images of thin section showing cracks and reactive fine aggregate, top half, plane polarized light, bottom half, epifluorescent mode.

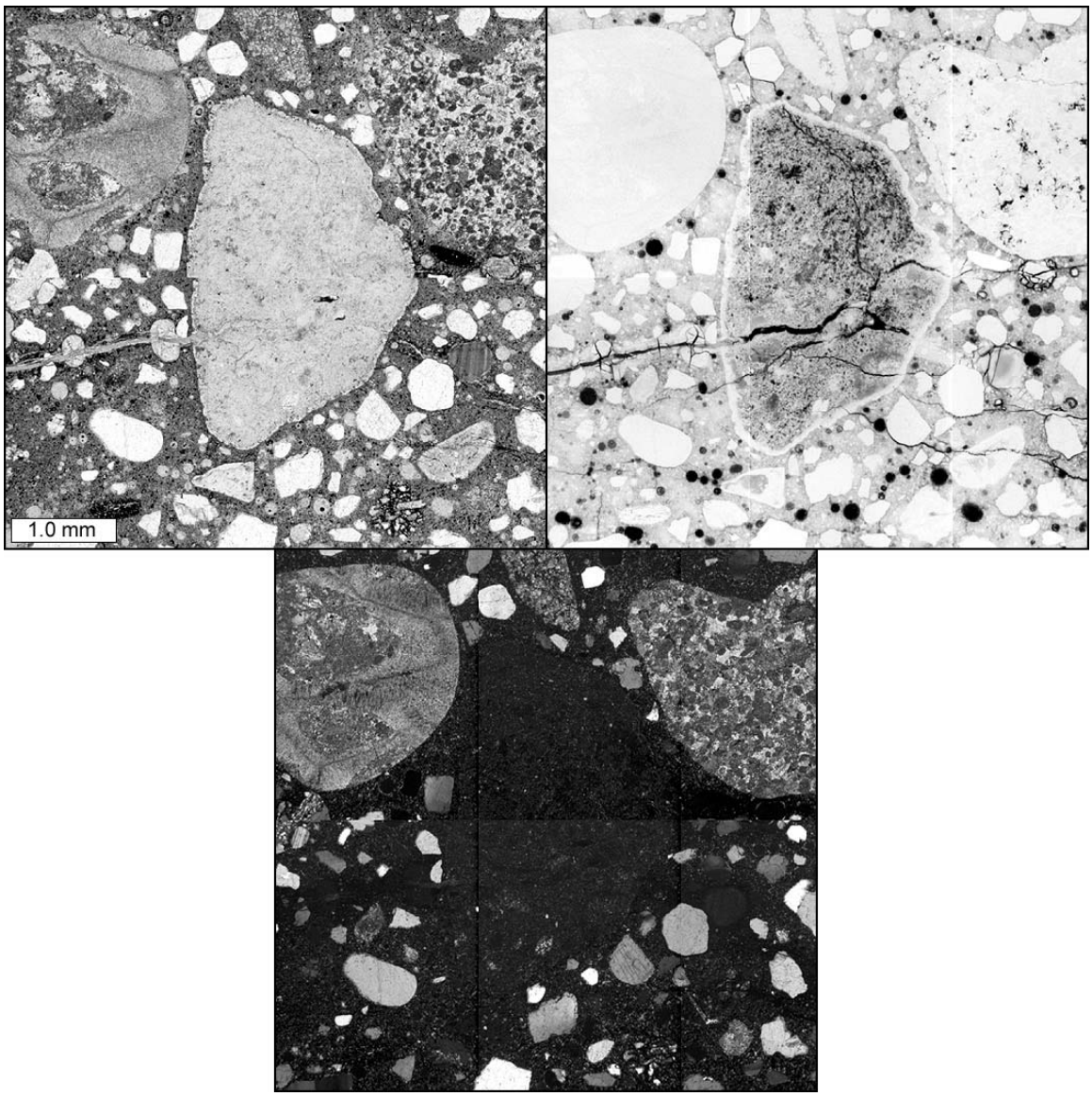

Figure 14: Close-up of reactive chert particle from upper left hand corner of Figure 13, clockwise from upper left: plane polarized light, epifluorescent mode, and crossed polarized light.

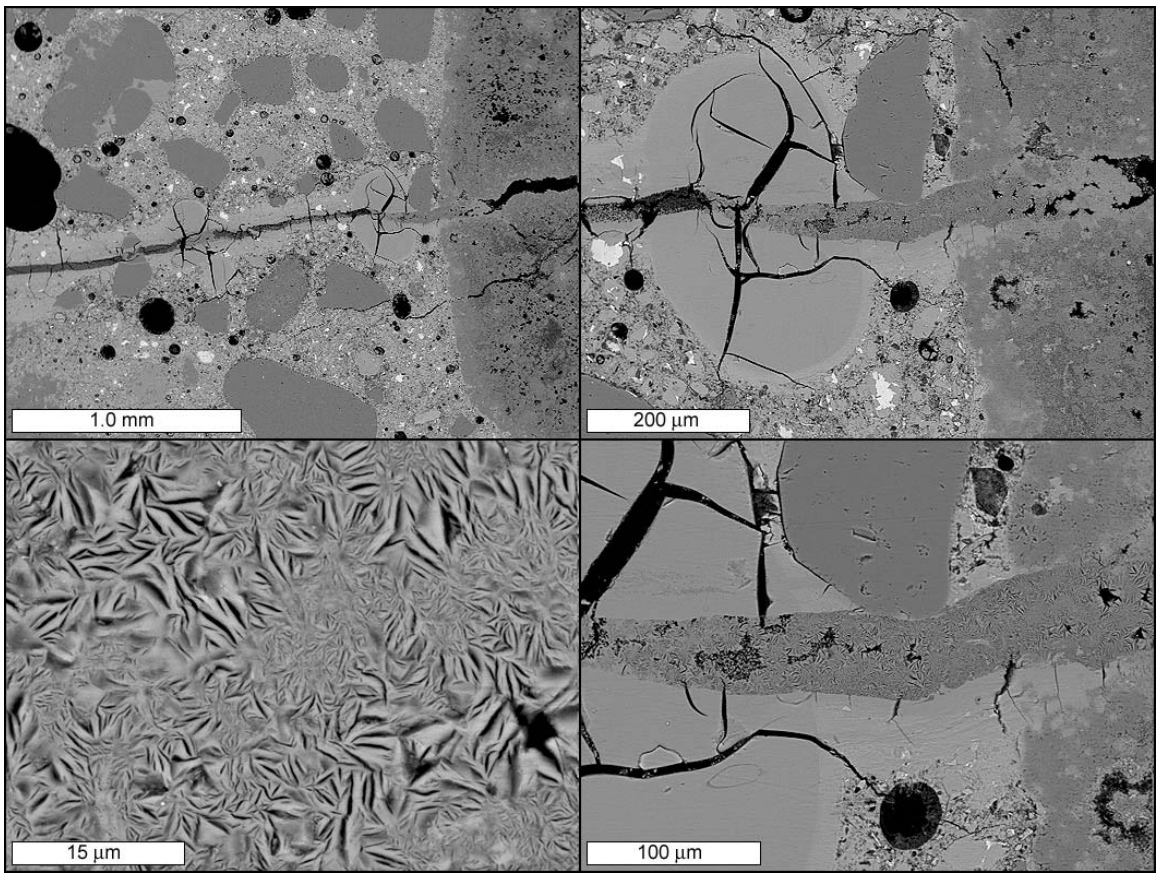

Figure 15: Backscattered-electron images of alkali-silica reaction product in crack from Figures 13 and 14, with successive close-ups to illustrate both the crystalline bladed and amorphous phases.

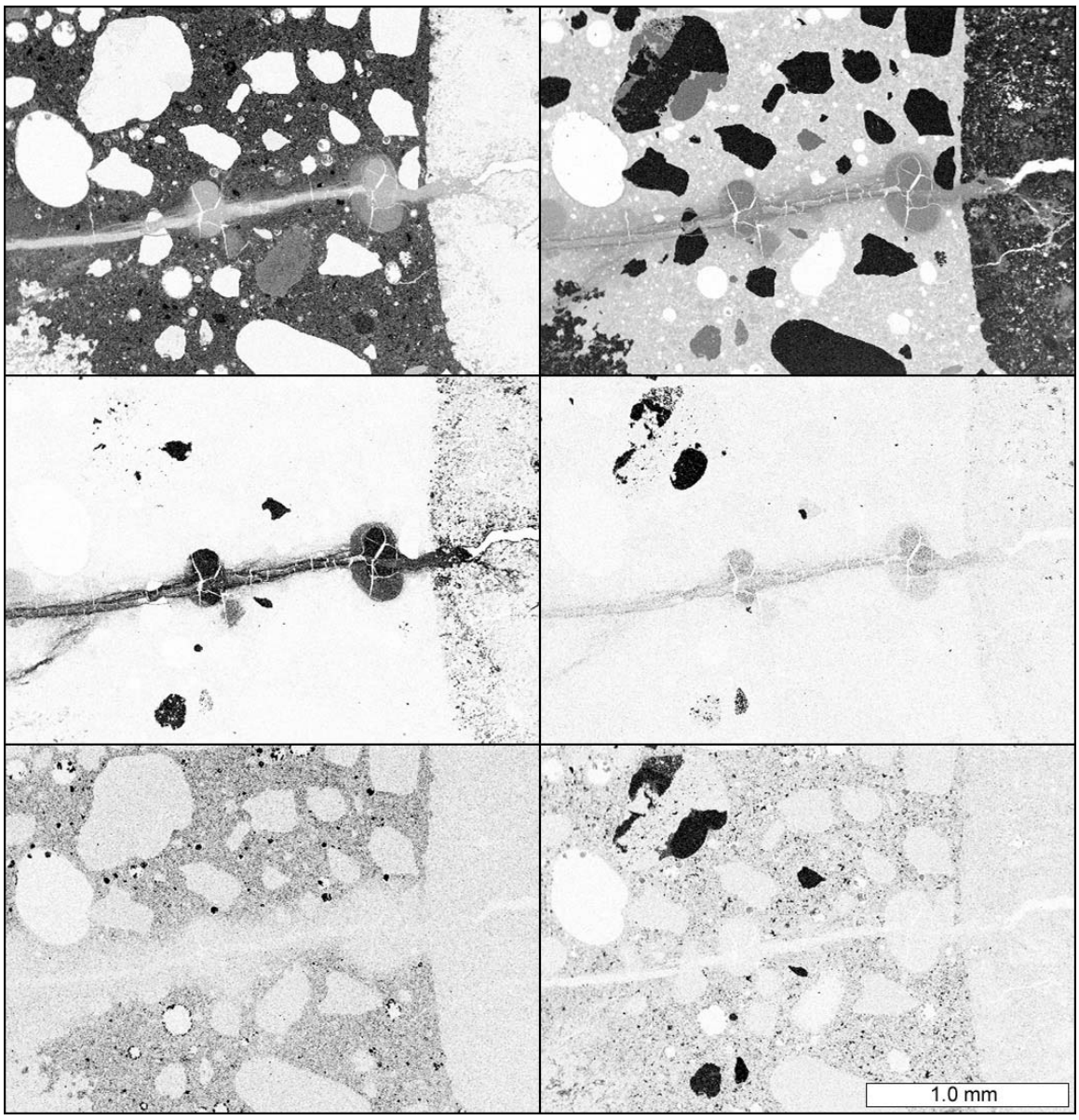

Figure 16: Elemental maps of characteristic Kα radiation, darker regions indicate higher counts for radiation, top row, from left to right, calcium and silicon, middle row, from left to right, potassium and sodium, bottom row, from left to right, sulfur and aluminum.

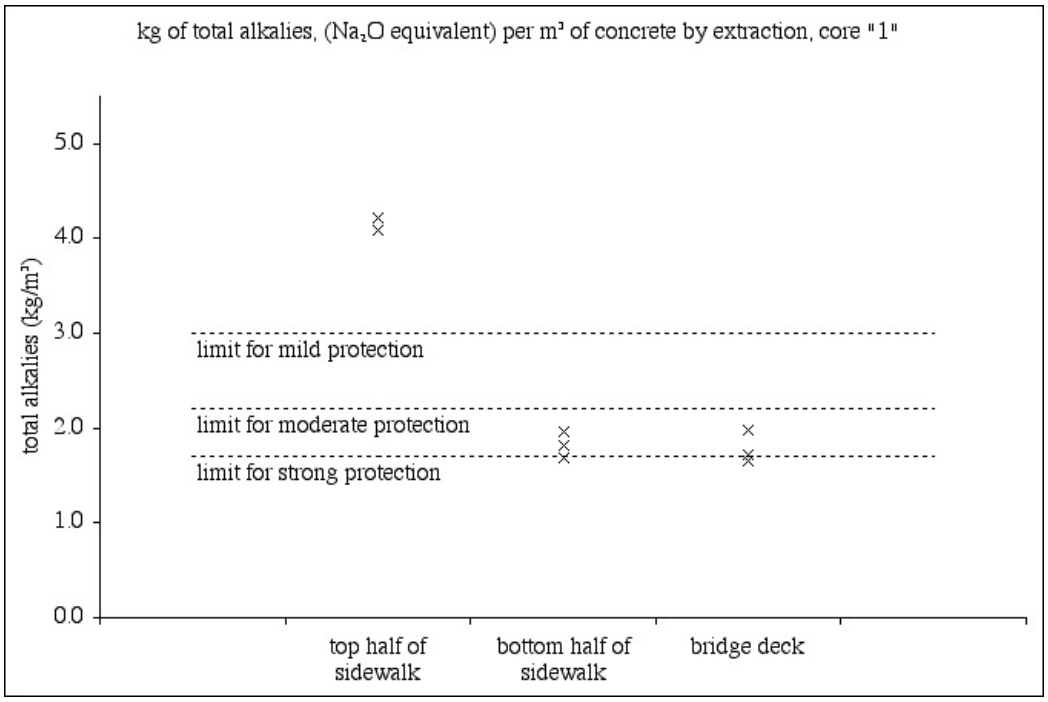

Figure 17: Plot of alkali extractions from core "1."

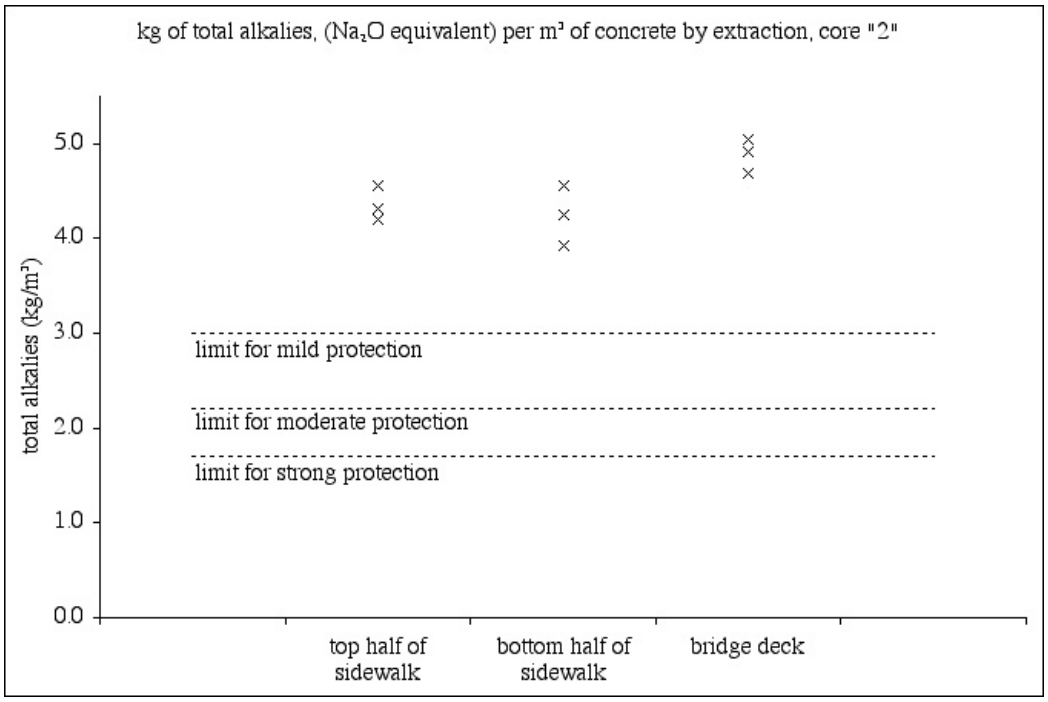

Figure 18: Plot of alkali extractions from core "2."

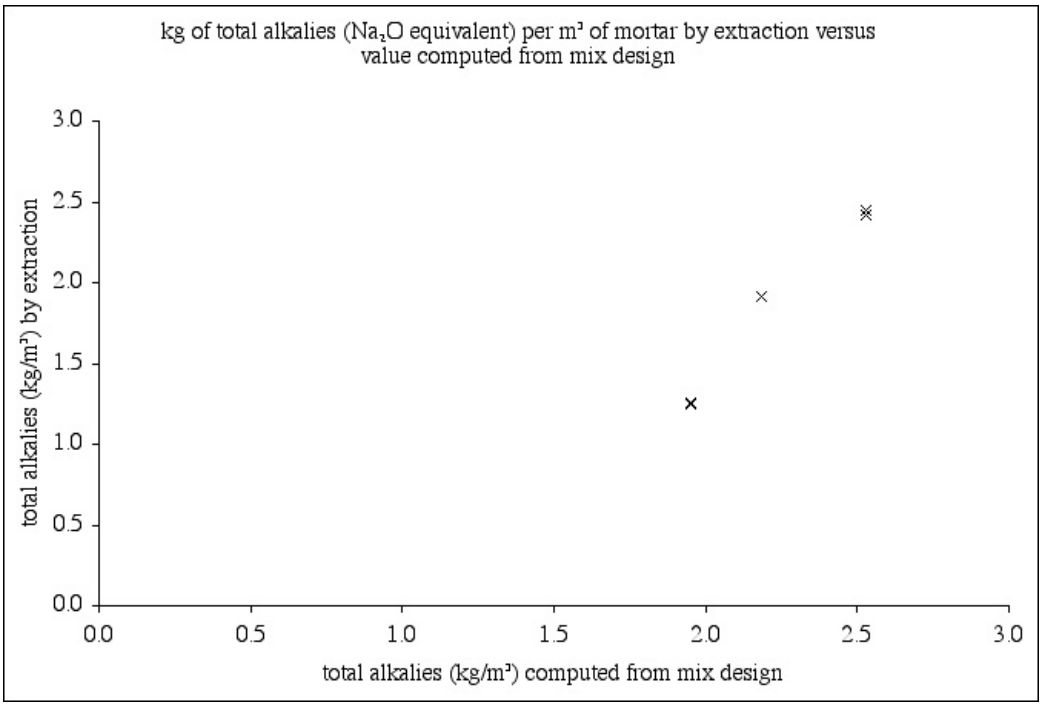

Figure 19: Plot of alkali extraction efficiency assessment results.